PHYSICAL REVIEW B VOLUME 49, NUMBER 12 15 MARCH 1994-II

Metastable vacancy in the *EL*2 defect in GaAs studied by positron-annihilation spectroscopies

K. Saarinen, S. Kuisma, and P. Hautojärvi
Laboratory of Physics, Helsinki University of Technology, 02150 Espoo, Finland

C. Corbel and C. LeBerre
Institut National des Sciences et Techniques Nucléaires, Centre d'Etudes Nucléaires de Saclay, 91191 Gif-sur-Yvette Cedex, France

(Received 27 October 1993)

We have performed positron-lifetime and Doppler-broadening experiments before and after illumination of undoped semi-insulating GaAs with 0.7–1.5-eV photons. When the *EL*2 defect is transformed to the metastable state by 1.1–1.3-eV photons, we observe a metastable vacancy defect. Its concentration is proportional to the *EL*2 concentration. The metastable vacancy has smaller open volume than isolated Ga and As vacancies and it is connected to a negative charge. The vacancy is generated with an optical cross section of 2×10^{-18} cm^2 at the photon energy of 1.15 eV and it recovers at 120 K. As these properties are identical to those of the metastable state of *EL*2, we conclude that the observed vacancy is involved in its atomic configuration. The results are in good agreement with the isolated As antisite model for the structure of the *EL*2 defect.

I. INTRODUCTION

The influence of native point defects on the electrical and optical properties of semiconductor material has been found particularly important in gallium arsenide. Especially the so-called *EL*2 defect in GaAs has been the object of extensive theoretical and experimental investigations.[1–3] This is mainly due to the technological importance of this defect: the *EL*2 center compensates the residual acceptor impurities and pins the Fermi level to the midgap position. As a result of this compensation process, semi-insulating GaAs can be manufactured without intentional impurity doping. However, in spite of the intensive research effort, the atomic nature of the *EL*2 defect is still a matter of controversy.

Much of the research interest in the *EL*2 center is motivated also by the exciting physical properties of this defect. Especially, the metastability of *EL*2 has been studied extensively. The metastable state of *EL*2 can be populated by illumination with 1.1–1.3-eV light at low temperatures of $T<100$ K. This state is electrically and optically inactive. The metastable state can be returned to the stable state by annealing at $T>120$ K, which corresponds to a thermal activation energy of about 0.3 eV. The metastable state recovers also optically by illuminating with 0.7- or 1.5-eV photons at temperatures within the range 70–100 K.[1–3]

Since the metastable state of *EL*2 is optically and electrically inactive, it has turned out to be difficult to obtain direct information on it by conventional defect spectroscopies like infrared absorption and deep-level transient spectroscopy. An electron level connected to the metastable state of *EL*2 has been detected only under hydrostatic pressure.[4–7] In electron-paramagnetic-resonance (EPR) measurements no signal of the metastable state can be obtained, because the defect is in a nonparamagnetic neutral charge state. On the other hand, the stable state of *EL*2 can be either neutral or positive, and the positive charge state has been detected in EPR measurements.[1–3,8] On the basis of these experiments, the *EL*2 defect has been related to the As antisite, i.e., the As atom on the Ga lattice site. However, it is not clear whether the As antisite appears in isolation or as a part of a larger defect complex.

Several atomic models have been developed for the *EL*2 defect and for its transition to the metastable state.[9–14] Generally, the metastable state is described as a local potential minimum induced by large lattice relaxations, which take place when the defect transforms from the stable to the metastable state. For example, in one of the models the *EL*2 defect is an As antisite bound to an As interstitial, which changes its lattice position in the metastable state.[12] More recently, it has been suggested that the *EL*2 defect consists of an isolated As antisite.[9,10] When the defect transforms to the metastable state, the As antisite atom moves from the substitutional lattice site towards the interstitial position. According to this model, an asymmetric Ga vacancy thus appears in the metastable state.[9,10]

In this work, we have applied positron-annihilation techniques to study the *EL*2 defect in semi-insulating (SI) GaAs. Positrons in solids are strongly repelled by the positive ion cores; thus, open-volume defects act as attractive centers, at which positrons can become localized. Since the electron density at these defects is lower than in the bulk, the lifetime of the positron at the open-volume center is larger than in the perfect crystal. Furthermore, the positron-electron momentum distribution narrows at a vacancy defect, which reduces the Doppler broadening of the 511-keV annihilation line. Consequently, positron-lifetime and Doppler-broadening experiments can be used to get information on vacancy-type defects on an atomic scale.[15,16]

The results of this work can be summarized as follows.

 ©1994 The American Physical Society

When the $EL2$ defect is transformed to the metastable state $EL2^*$, we observe a metastable vacancy. This vacancy has a smaller open volume than isolated Ga and As vacancies. It is generated with the same optical cross section as the metastable state of the $EL2$ defect, and its recovery kinetics are identical to those of $EL2^*$. The concentration of the metastable vacancy is proportional to the $EL2$ concentration. We conclude that the metastable state of $EL2$ involves the vacancy. The results are in perfect agreement with the isolated As antisite model for the $EL2$ defect.

This paper completes our preliminary results of the $EL2$ defects in GaAs.[17,18] The experimental details are described in Sec. II, and the results are given in Sec. III. The data analysis with the positron trapping model is explained in Sec. IV. In Sec. V we compare the observed vacancy properties to those of the $EL2$ defect. Section VI concludes the paper.

II. EXPERIMENTAL DETAILS

The positron and infrared-absorption experiments of this work were performed on five undoped semi-insulating GaAs crystals, which were grown by the liquid-encapsulated Czochralski (LEC) technique. The resistivity of the samples was about $10^8\ \Omega\,\text{cm}$, and their $EL2$ concentration was typically $10^{16}\ \text{cm}^{-3}$. The samples and their $EL2$ concentrations are listed in Table I. The $EL2$ concentrations were determined either by infrared-absorption or EPR techniques, and these numbers indicate the amount of the defect in the neutral charge state $EL2^0$. Only in sample 5 have we the more detailed information $[EL2^0]=[EL2^+]=1.0\times10^{16}\ \text{cm}^{-3}$, obtained by EPR experiments.[19]

The infrared-absorption experiments were performed by measuring the light transmission with a calibrated Ge photodetector. Monochromatic light with photon energies of 0.7–1.5 eV was made to hit the sample in a closed-cycle He cryocooler equipped with quartz glass windows for the incident and transmitted light fluxes. The intensity of the incident light was monitored on line using a bifurcated optical-fiber bundle and a Si-Ge photodetector.

The positron-lifetime and Doppler-broadening experiments were performed in a conventional way.[15,16] Two identical sample pieces were sandwiched with a 30-μCi positron source. The source material was carrier-free ^{22}NaCl deposited on a 1.5-μm Al foil. The sample sandwich was mounted in a closed-cycle He cryocooler for positron experiments at 20–300 K. The cryostat was equipped with quartz glass windows allowing the illumination of the sample together with positron experiments. The illuminations were performed either with white light or with 0.7–1.5-eV light obtained from a 250-W halogen lamp and a monochromator. The source-sample sandwich was illuminated simultaneously from both sides using a trifurcated optical-fiber bundle. The reference fiber bundle was used for on-line monitoring of the incident photon flux with a Si-Ge photodetector.

The positron-lifetime measurements were carried out by a fast-fast lifetime spectrometer with a time resolution of 230 ps. Roughly 2×10^6 counts were collected for each spectrum within the typical counting time of 3 h. After subtracting the coincidence background and the annihilations in the source materials (215 ps, 5.4%; 450 ps., 1.9%), the lifetime spectra were analyzed with one or two exponential components:

$$n(t)=n_0[I_1\exp(-\lambda_1 t)+I_2\exp(-\lambda_2 t)]\ , \tag{1}$$

convoluted with the Gaussian resolution function of the spectrometer. In Eq. (1), n_0 is the total number of observed annihilation events, and the annihilation rate λ_i is the inverse of the positron lifetime, $\lambda_i=\tau_i^{-1}$. I_i in Eq. (1) denotes the relative intensity of the lifetime component τ_i in the spectrum. The values of the lifetimes τ_i and intensities I_i can be used to calculate the positron average lifetime

$$\tau_{av}=I_1\tau_1+I_2\tau_2\ . \tag{2}$$

This parameter is insensitive to the uncertainties in the decomposition procedure and coincides with the center of mass of the lifetime spectrum.

The Doppler broadening of the annihilation radiation was recorded simultaneously with the lifetime experiments by a high-purity Ge γ detector with an energy resolution of 1.2 keV. Typically 10^7 counts were collected to the 511-keV annihilation line. The shape of the 511-keV line was described by the conventional line-shape parameters S and W.[15,16] The S parameter is the relative number of annihilation events around the 1.4-

TABLE I. The samples studied in this work and their $EL2$ concentrations. The $EL2$ concentration corresponds to the neutral charge state $EL2^0$ only. The positron average lifetime τ_{av} is shown both in darkness before illumination of the sample and after illumination with 1.2-eV photons for 1 h with a flux of $10^{16}\ \text{s}^{-1}\,\text{cm}^{-2}$. Both values have been measured at 25 K. The statistical error of the average lifetime is about 0.3 ps in all measurements.

Sample	Concentration of $EL2$ defects (cm^{-3})	Positron average lifetime in darkness (ps)	Positron average lifetime after illumination (ps)
1	4.6×10^{16}	237.3	241.8
2	2.5×10^{16}	234.4	240.0
3	1.2×10^{16}	232.0	237.0
4	1.0×10^{16}	232.4	234.9
5	1.0×10^{16}	230.8	233.8

keV-wide central region of the peak. The W parameter is calculated from the tail of the peak at the energy range of $\pm(2.55-4.08$ keV) from the centroid. The S parameter (the valence annihilation parameter) represent mainly positron annihilation with low-momentum valence electrons, whereas only annihilations with the core electrons fall in the energy window of the W parameter (the core annihilation parameter).

III. EXPERIMENTAL RESULTS

A. Infrared-absorption experiments

Infrared-absorption measurements were used to study the well-known photoquenching and annealing properties of the $EL2$ defect in semi-insulating GaAs. In the infrared-absorption spectrum of sample 1, the absorption coefficient started to increase at a photon energy of about $E_{ph}=0.7$ eV. The increase became stronger at $E_{ph}=1.0-1.2$ eV, and a local maximum was obtained at about $E_{ph}=1.2$ eV. At higher photon energies the absorption coefficient increased further, until the absorption due to the GaAs energy gap was seen at about $E_{ph}=1.5$ eV.

The infrared-absorption spectrum of sample 1 was found to be remarkably similar to that observed in earlier studies.[1,20] The spectrum can be explained by optically induced electron transfers between the bands and the $EL2$ energy levels in the gap.[1,21] Hence, we conclude that $EL2$ defects are present in our samples and that they dominate the absorption spectrum at photon energies below the width of the band gap.

The effect of photoquenching the $EL2$ defects was also studied in the infrared-absorption experiments. As a function of the illumination time, the absorption coefficient at $E_{ph}=1.1-1.3$ eV decreased monotonically toward zero. The effect was fastest at a photon energy of $E_{ph}=1.15$ eV, at which energy an illumination time of 400 s with the flux $\Phi=10^{15}$ s^{-1}cm^{-2} was needed to decrease the absorption coefficient to half of its original value. At photon energies of $E_{ph}<1.1$ eV no photoquenching effects were observed, and at $E_{ph}>1.3$ eV the decrease of the absorption coefficient became very slow. For example, at $E_{ph}=1.4$ eV the half-time is about 3000 s when a photon flux of $\Phi=10^{15}$ s^{-1}cm^{-2} is applied. After all illumination treatments, the original ir-absorption was restored by thermal annealing at 120 K (see Sec. III B).

The photoquenching characteristics of the ir-absorption were exactly similar to those reported earlier, and the photoquenching is a well-known property of the $EL2$ defect.[1-3] It results from the disappearance of the $EL2$ electron levels from the energy gap, when the defect is converted to the metastable state by illumination. Above 120 K the metastable state is no longer thermally stable, and the original ir-absorption is restored, since the $EL2$ electron levels appear again in the band gap. The time dependence of the photoquenching can be converted to the optical cross section for the transition between stable and metastable states of $EL2$. This analysis will be explained in detail later in this paper in connection with the positron-annihilation data (Sec. V).

B. Positron-annihilation results: Photoquenching and thermal annealing

When measured in darkness, the positron average lifetime at 300 K is very close to the bulk value of $\tau_b=231$ ps. At low temperatures, the average lifetime increases to about 232–238 ps depending on the sample. The positron lifetimes measured in darkness at 25 K are collected for all samples in Table I.

Table I shows further the positron average lifetime τ_{av} in darkness at 25 K after 1-h illumination with white light or with 1.2-eV monochromatic light. The effect is clear: after illumination the positron lifetime in all samples is longer than the reference levels obtained in darkness. The increase varies from 2 to 6 ps depending on the sample. Furthermore, the increase of the positron lifetime is persistent, i.e., when the sample is kept at 25 K, the change of τ_{av} remains permanently even if the illumination is turned off. The change of positron lifetime is the same independent of whether the illumination is performed with white light or with 1.2-eV monochromatic light. The illumination effect is observed also in the Doppler line-shape parameters S and W. For example in sample 2, the S parameter increases by 0.43% and the W

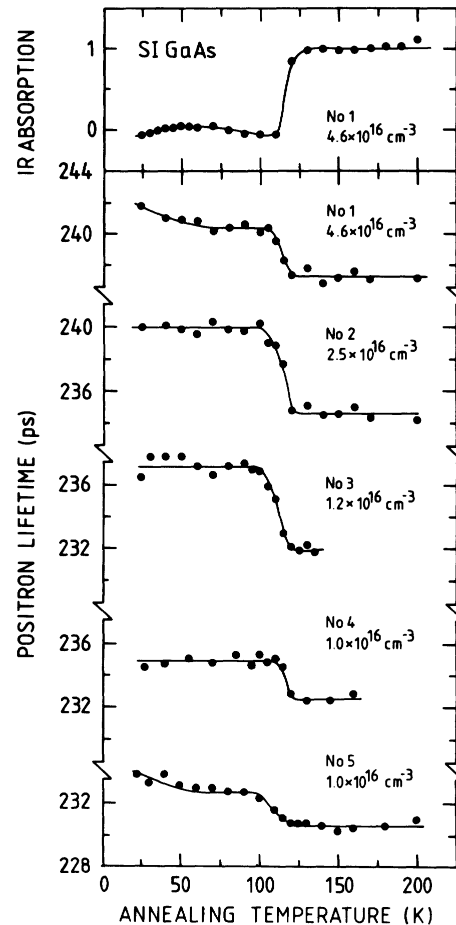

FIG. 1. Normalized ir absorption coefficient in sample 1 and the average positron lifetime as functions of isochronal annealing temperature after illumination with 1.2-eV photons. All the measurements were performed in darkness at 25 K. The $EL2$ concentrations of the samples are marked in the figure.

parameter decreases by 2.0% after illumination.

The effects of 10-min isochronal annealings on the positron lifetime are shown in Fig. 1. The experiments were performed at 25 K after 1-h illumination with 1.2-eV light at a typical photon flux of $\Phi = 10^{16}$ s^{-1} cm^{-2}. Figure 1 shows further the infrared-absorption coefficient at 1.2 eV as a function of the annealing temperature. As seen in the ir data, the absorption at 1.2 eV becomes very small after illumination, indicating that the $EL2$ defects have been totally transformed to the metastable state. At 120 K the absorption recovers, when the metastable state of $EL2$ anneals out. This curve is in good agreement with the results of previous ir-absorption experiments.[1,2,3,22]

In all samples, the annealing curves of the positron parameters behave in the same way. The higher values of positron average lifetime obtained after illumination at 25 K remain up to 110 K, but at about 120 K an abrupt decrease is observed in the data. After this stage the positron average lifetime saturates at the level corresponding to the situation before illumination. A small recovery stage is observed also at 40–50 K in some samples.

The results of the Doppler-broadening experiments after illumination of the samples are shown as a function of the annealing temperature in Fig. 2. The results are scaled to the S- and W- parameter values measured in darkness before illumination. In Fig. 2 the line-shape parameters S and W are constant up to about 110 K. At 110–120 K, the S parameter decreases and the W parameter increases, after which both parameters saturate to the values obtained before illumination. Hence, the line-shape parameters S and W behave analogously to the average lifetime, and the observed illumination effects recover at 120 K.

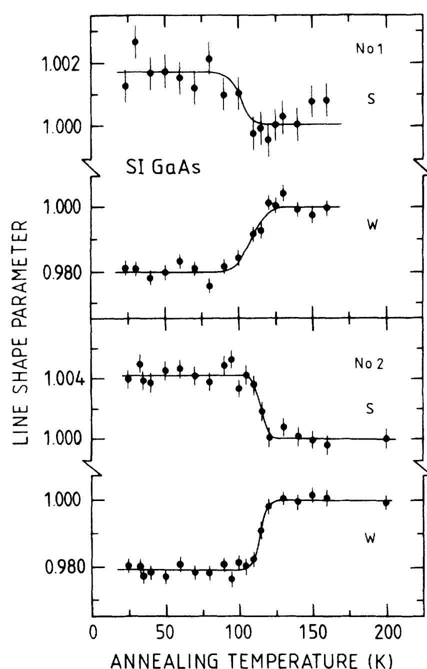

FIG. 2. Positron-annihilation line-shape parameters S and W as functions of isochronal annealing temperature in samples 1 and 2 after 1.2-eV photon illumination. All measurements were performed in darkness at 25 K.

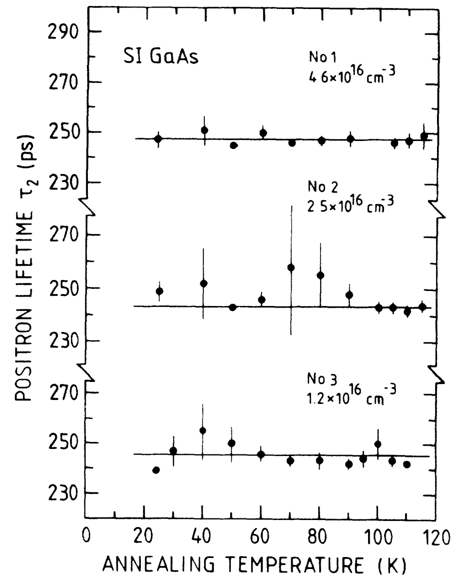

FIG. 3. Lifetime component τ_2 from the decomposition of the lifetime spectra as a function of isochronal annealing temperature in samples 1, 2, and 3. The two-component analysis has been performed on the data of Fig. 1.

After illumination with 1.2-eV light the lifetime spectra can be decomposed to two components. Figure 3 shows the longer-lifetime component τ_2 from this analysis as a function of the annealing temperature of the sample, i.e., from the same experiments as τ_{av} in Fig. 1. The values of τ_2 are scattered in the range 240–255 ps in all samples, and the intensity of this component is typically 80–90 %. Hence, the decomposition of the lifetime spectra gives a longer component of $\tau_2 = 247 \pm 3$ ps after the 1.2-eV light illumination.

To study in more detail the kinetics of the annealing stage at 120 K, we have performed an isothermal annealing experiment with sample 2.[17] The time for the 50% recovery was determined by positron-lifetime and infrared-absorption measurements during annealings at 120, 115, 110, and 106 K. When the temperature was increased from 106 to 120 K, the time required for the 50% recovery of the positron lifetime changed from 28 000 to 270 s. Both ir-absorption and positron experiments gave consistent recovery times, and the same apparent activation energy of $E_A = 0.36 \pm 0.03$ eV could be determined for the recovery process using both techniques.[17]

We have observed also an optically assisted recovery of the positron lifetime.[17] Sample 2 was first photoquenched with 1.2-eV light at 25 K, after which it was illuminated at 80 K with a 10-W halogen lamp and a heat-absorbing filter of about 1% transmittance for 1.4-eV photons. During 32-h illumination at 80 K, the average positron lifetime measured at 25 K decreased continuously from $\tau_{av} = 240$ ps to 234 ps, which is the reference level observed at 25 K before illumination.

C. Generation of the illumination effect

After illumination with white light or 1.2-eV light, the positron lifetime at 25 K increases persistently. To study

in detail the generation of this illumination effect, we have used a monochromatic 0.7–1.5-eV light source with an adjustable photon flux. This allows us to determine the optical cross section corresponding to the permanent illumination effect on the positron lifetime.

The positron average lifetime in sample 1 as a function of the illumination time is shown in Fig. 4. The experiments were performed in darkness at 25 K after illumination with 1.15-eV photons at a constant photon flux of $\Phi=10^{14}$ $s^{-1}cm^{-2}$. As a function of the illumination time, the positron average lifetime increases first steeply within the time range 0–2000 s. Then, the increase of τ_{av} saturates exponentially, and 80% of the saturation effect is obtained after about 5000 s of illumination.

In Fig. 5 we have studied the persistent illumination effect in sample 1 as a function of the photon energy. All experiments were performed at 25 K in darkness after the illumination, and after each experimental point the sample was annealed at 200 K to remove the illumination effect completely (see Sec. III B). In all experiments, the photon flux was $\Phi=5\times10^{14}$ $s^{-1}cm^{-2}$ and the illumination time was 900 s.

As seen in Fig. 5, there is no illumination effect at photon energies $E_{ph}<1.05$ eV. However, at $E_{ph}\geq1.05$ eV the curve rises steeply, and the maximum effect is obtained at $E_{ph}=1.15$ eV. At higher photon energies the positron lifetime decreases monotonically, and a spectrum peak centered at 1.15 eV is thus obtained. The full width at half maximum of this peak is about 0.2 eV. In conclusion, a persistent increase in positron lifetime can be obtained with either white light or monochromatic light of photon energies 1.1–1.3 eV. The effect is strongest when the illumination is performed with 1.15-eV photons.

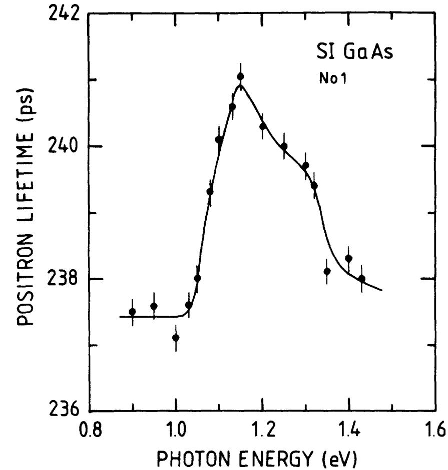

FIG. 5. Average positron lifetime as a function of the photon energy in sample 1. The spectra were measured in darkness after illumination of the sample with a photon flux of 5×10^{14} $s^{-1}cm^{-2}$ for 900 s. Measurement temperature was 25 K.

D. Temperature dependence of the positron lifetime

After illuminating the sample at 25 K with 1.1–1.3-eV light, the positron lifetime can be studied as a function of the measurement temperature in the range 20–100 K, i.e., at temperatures below the observed main annealing stage at 120 K. The results of such experiments are shown in Fig. 6. Before the positron measurements in darkness the samples were illuminated at 25 K with 1.2-eV light for 1 h with a typical photon flux of $\Phi=10^{16}$ $s^{-1}cm^{-2}$. Figure 6 shows further the positron lifetimes measured in darkness before illumination. All curves in Fig. 6 were reversible as a function of temperature.

The positron average lifetime in darkness before illumination increases at low temperatures. After il-

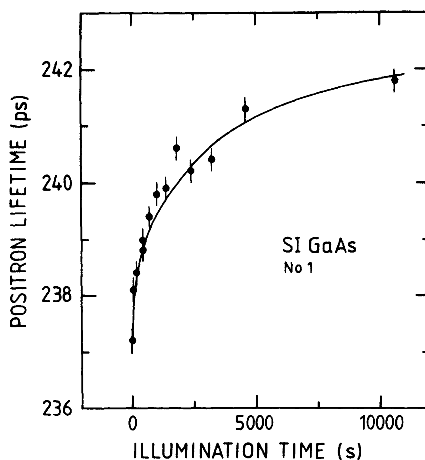

FIG. 4. Average positron lifetime as a function of illumination time in sample 1. A photon energy of 1.15 eV and a photon flux of 10^{14} $s^{-1}cm^{-2}$ were used in illumination. Positron-lifetime spectra were measured in darkness at 25 K after each illumination.

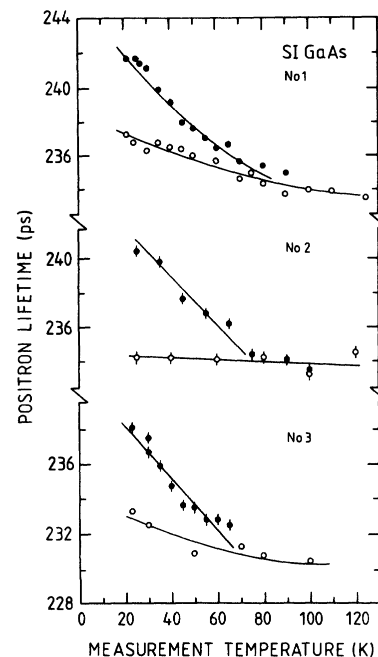

FIG. 6. Average positron lifetime as a function of measurement temperature in samples 1, 2, and 3. The spectra measured in darkness after 1.15-eV illumination are marked with closed circles and the reference level with open circles.

lumination with 1.2-eV light, τ_{av} increases persistently. However, this illumination effect depends strongly on the measurement temperature (Fig. 6). When the temperature is increased, the positron average lifetime decreases strongly in all samples. At about 70 K, the illumination effect can hardly be detected because τ_{av} almost coincides with the reference level. Hence, below the *annealing* temperature of 120 K, the illumination effect observed in positron parameters depends strongly on the *measurement* temperature: at low temperatures the persistent change of τ_{av} is clearly enhanced.

IV. POSITRON TRAPPING AT VACANCY DEFECTS

In a defect-free crystal, positrons are delocalized and annihilate with a single lifetime τ_b. When open-volume defects like vacancies are present in the material, positrons may become localized at them and annihilate with another lifetime τ_v. Because the electron density in a vacancy is lower than in the bulk, the lifetime τ_v is always longer than the bulk lifetime τ_b. The positron trapping rate κ_v from the delocalized state into the vacancy is proportional to the vacancy concentration c_v:

$$\kappa_v = \mu_v c_v \ , \tag{3}$$

where μ_v is the positron trapping coefficient. For negative vacancies μ_v is roughly $2\times10^{15}\ \mathrm{s}^{-1}$ at 300 K, and it increases by an order of magnitude when the temperature is decreased to 20 K.[23–25] Positron trapping at neutral vacancies is independent of temperature, and the trapping coefficient is typically $\mu_v = 1\times10^{15}\ \mathrm{s}^{-1}$.[23–25] At positive vacancies the trapping coefficient is several orders of magnitude smaller, due to the Coulomb repulsion between the defect and the positron.[25]

The positron average lifetime τ_{av} is a superposition of the lifetimes in the bulk τ_b and at the vacancy defects τ_{vi}:

$$\tau_{av} = \eta_b \tau_b + \sum_i \eta_{vi} \tau_{vi} \ , \tag{4}$$

where η_b and η_{vi} are the fractions of positron annihilations in the bulk and at the vacancies of type i, respectively. A similar equation can be written also for the line-shape parameters S and W. In the positron trapping model,[26] the fractions η_b and η_{vi} are related to the trapping rates κ_{vi} at the vacancy i by the following formulas:

$$\eta_b = \lambda_b \Big/ \left[\lambda_b + \sum_i \kappa_{vi} \right] , \tag{5}$$

$$\eta_{vi} = \kappa_{vi} \Big/ \left[\lambda_b + \sum_i \kappa_{vi} \right] , \tag{6}$$

where $\lambda_b = \tau_b^{-1}$ is the positron-annihilation rate in the bulk. When vacancies with $\tau_{vi} > \tau_b$ are present in the sample, $\kappa_{vi} > 0$ and $\eta_{vi} > 0$, yielding $\tau_{av} > \tau_b$ through Eq. (4). Hence, the increase of the positron average lifetime above the bulk level is always a clear sign that vacancy defects are present in the samples. Furthermore, when the measured τ_{av} increases compared to its earlier value, more positron trapping at vacancies is taking place in the sample than previously.

The vacancy defect revealed by the increase of positron average lifetime can be further characterized by the information obtained from the decomposition of the lifetime spectra. If only one type of vacancy with the positron lifetime τ_v is dominant in the sample, the experimental component τ_2 is equal to the lifetime corresponding to this positron trap: $\tau_v = \tau_2$. In this case the positron trapping rate can be calculated from Eqs. (4)–(6) by

$$\kappa_v = \lambda_b \frac{\tau_{av} - \tau_b}{\tau_v - \tau_{av}} \ , \tag{7}$$

and the defect concentration can be obtained from Eq. (3). However, when two vacancy traps coexist in the sample and a two-component analysis of the lifetime spectra is performed, the experimental lifetime τ_2 becomes the superposition of the two lifetimes at vacancy defects[27]

$$\tau_2 = \frac{I_{v1}\tau_{v1} + I_{v2}\tau_{v2}}{I_{v1} + I_{v2}} \ , \tag{8}$$

where I_{v1} and I_{v2} are the intensities corresponding to the lifetimes τ_{v1} and τ_{v2}, respectively. When the total trapping rate $\kappa = \kappa_{v1} + \kappa_{v2}$ is much larger than $(\lambda_b - \lambda_{v1})$ or $(\lambda_b - \lambda_{v2})$, Eq. (8) becomes[27]

$$\tau_2 = \frac{\kappa_{v1}}{\kappa_{v1} + \kappa_{v2}} \tau_{v1} + \frac{\kappa_{v2}}{\kappa_{v1} + \kappa_{v2}} \tau_{v2} \ . \tag{9}$$

In this case the total trapping rate $\kappa = \kappa_{v1} + \kappa_{v2}$ can be calculated from Eq. (7) by substituting $\tau_v = \tau_2$. Equation (9) can also be used, for example, to estimate the value of τ_{v2}, if the total trapping rate $\kappa = \kappa_{v1} + \kappa_{v2}$ is calculated from Eq. (7) and the values of κ_{v1} and τ_{v1} are known.

V. METASTABLE VACANCY AND THE *EL*2 DEFECT

We can summarize our experimental findings described in Sec. III as follows. (i) We have observed that positron lifetime increases persistently after illuminating the sample at 25 K. (ii) The increase can be generated by photons in the energy range $E_{ph} = 1.1-1.3$ eV, and the effect is strongest with the photon energy of $E_{ph} = 1.15$ eV. (iii) The persistent increase of positron lifetime recovers at 120 K. (iv) The magnitude of the persistent change of positron lifetime is strongly temperature dependent.

In this section we shall analyze these results further in terms of the positron-trapping model presented in Sec. IV. We shall examine especially the relation of the positron results to those of the infrared-absorption experiments, and discuss the information that the present positron data provide on the structure of the *EL*2 defect.

A. Positron trapping at the metastable vacancy

In the samples studied in this work, the positron lifetime in darkness is at low temperatures clearly above the bulk level, and it decreases as a function of temperature. This behavior indicates the presence of native vacancy defects, which are in a negative charge state. The second lifetime component is $\tau_2 = 250-260$ ps, which is typical for monovacancies in GaAs.[27–31] In our recent work,

these defects have been identified as native Ga vacancies.[32] By using the positron trapping coefficient of $\mu_v = 1.5\times10^{15}$ s^{-1} at 300 K obtained previously for irradiation-induced Ga vacancies[29] and scaling to low temperatures,[24,32] we estimate from Eqs. (3) and (7) that the Ga-vacancy concentration varies in the range $(2-12)\times10^{15}$ cm^{-3} in the samples studied in this work.

When the SI GaAs samples are illuminated at 25 K, the positron average lifetime increases persistently (Sec. III). On the basis of the discussion presented above in Sec. IV, this indicates that more positron trapping takes place at vacancy defects after illumination when compared to the measurements of the sample in darkness. Hence, a new vacancy defect is generated in the sample during illumination at the low temperature of 25 K. When the illumination is removed, the vacancy can be observed persistently, until thermal annealing is performed at about 120 K (Fig. 1). This behavior indicates that the vacancy possesses metastable character.

The second lifetime component after illumination of the sample is $\tau_2 = 247\pm3$ ps (Fig. 3). As explained above, a new type of vacancy defect is revealed after illumination of the sample by the increase of the positron average lifetime. Therefore, two types of vacancies may trap positrons after illumination: the Ga vacancies found already in the darkness before illumination of the sample and the metastable vacancies observed after illumination. In this case, the second lifetime τ_2 is the superposition of the lifetimes at Ga vacancies $\tau_{V_{Ga}} = 260$ ps (Ref. 29–32) and at the metastable vacancies with the positron lifetime τ_{v^*} (Eq. 8). Because the positron lifetimes after illumination are in samples 1–3 typically ≥ 10 ps above the bulk lifetime (228 ps at 25 K), Eq. (9) is also valid and the total trapping rate $\kappa = \kappa_{V_{Ga}} + \kappa_{v^*}$ can be obtained from Eq. (7) using $\tau_v = \tau_2$. The positron trapping rate at Ga vacancies $\kappa_{V_{Ga}}$ can be calculated from the data measured in darkness before illumination by using Eq. (7) with $\tau_v = 260$ ps. The trapping rate at the metastable vacancy κ_{v^*} can then be obtained from the total trapping rate as $\kappa_{v^*} = \kappa - \kappa_{V_{Ga}}$ by assuming that positron trapping at the Ga vacancies remains the same after as before illumination. Finally, the trapping rates can be used to estimate the positron lifetime τ_{v^*} at the metastable vacancy from Eq. (9). We have performed this analysis for the data obtained in samples 1–3, and in all of them we obtain consistently the positron lifetime value of $\tau_{v^*} = 245\pm3$ ps, corresponding to positrons annihilating at the metastable vacancy.

The positron lifetime $\tau_{v^*} = 245$ ps at the metastable vacancy defect is less than the values determined previously for the native Ga (260 ps) and As (257 or 295 ps) vacancies,[27,28] or for the Ga vacancies introduced by electron irradiation.[29,30] The positron lifetime at the vacancy is proportional to the open volume of the defect, which is determined by the defect geometry and the lattice relaxations.[31] Hence, the low lifetime $\tau_{v^*} = 245$ ps at the vacancy after illumination indicates that the open volume connected to this metastable vacancy is less than that observed typically for a monovacancy in GaAs.

The line-shape parameters corresponding to the metastable vacancy can be obtained from the Doppler-broadening data as follows. We assume that after illumination positrons are trapped at native Ga vacancies with $\tau_{V_{Ga}} = 260$ ps and at metastable vacancies with $\tau_{v^*} = 245$ ps. Then, we can calculate the positron trapping rates at V_{Ga} from Eq. (7) and at the metastable vacancy using Eqs. (4)–(6). For the native Ga vacancy we have determined the line-shape parameters of $S_{V_{Ga}}/S_b = 1.027(2)$ and $W_{V_{Ga}}/W_b = 0.87(1)$. Using these values and the positron-trapping rates we can calculate the line shape parameters S_{v^*} and W_{v^*} for the metastable vacancy by replacing the positron lifetimes in Eq. (4) by the corresponding S and W parameters. This analysis gives us the ratios $S_{v^*}/S_b = 1.011(2)$ and $W_{v^*}/W_b = 0.94(1)$ for the metastable vacancy. These values are smaller than those we have determined for native Ga or As vacancies ($S_v/S_b = 1.015-1.03$ and $W_v/W_b = 0.80-0.90$) or for Ga vacancies observed after electron irradiation ($S_v/S_b = 1.015$ and $W_v/W_b = 0.89$). The Doppler-broadening data are thus consistent with the results of the lifetime experiments in the respect that the open volume of the metastable vacancy is less than in isolated Ga or As monovacancies.

To summarize, the analysis of this section shows that the increase of positron lifetime after illumination of SI GaAs at 25 K can be related to the generation of a new vacancy defect. This vacancy is metastable in the sense that the vacancy can be induced by illumination only below 100 K and disappears during annealing at 120 K. The experimental results show further that the open volume of the metastable vacancy is less than in Ga or As vacancies. In the following sections, we investigate in detail the properties of this metastable vacancy, and correlate them to those of the *EL*2 defect.

B. Thermal stability of the metastable vacancy

In our experiments, the positron lifetime was increased persistently by light illumination at 25 K. In the isochronal annealings (Fig. 1), the original level of the positron lifetime was restored at 120 K. The infrared-absorption experiments show that the absorption due to the *EL*2 defect becomes negligible after the same illumination treatment (Fig. 1). The infrared-absorption coefficient stays at a low level up to 120 K, after which it retains its original value. The ir absorption and the positron lifetime behave thus in a strikingly similar way as functions of the annealing temperature.

The low level of the ir absorption after illumination is due to the photoquenching of the *EL*2 defects. During illumination with white light or with 1.1–1.3-eV light, the *EL*2 defects transform from the stable state to the metastable state *EL*2*, which does not absorb ir light.[1–3] The metastable state is thermally stable only below 120 K.[1–3] In the positron experiments, the appearance of the metastable vacancy thus correlates well with the transformations of *EL*2 between the stable and metastable states. When the ir absorption shows photoquenching of the *EL*2 defects, a metastable vacancy is detected in the positron-annihilation experiments. Furthermore,

when the metastable state of $EL2$ recovers at 120 K according to ir experiments, the metastable vacancy defect disappears also from the positron-annihilation data.

The kinetics of the annealing stage at 120 K can be studied in more detailed with isothermal annealing experiments. In positron-lifetime experiments the activation energy of $E_A = 0.36 \pm 0.03$ eV was determined for the recovery process in sample 2.[17] This value is very close to those reported earlier for annealing of the metastable state of the $EL2$ defect.[1–3,22] Furthermore, the ir-absorption measurements in sample 2 yield the same activation energy of $E_A = 0.36$ eV for the recovery of $EL2$ after photoquenching.[17] We can thus conclude that a metastable vacancy is observed when $EL2$ is photoquenched. This vacancy exhibits exactly the same annealing kinetics as the metastable state of the $EL2$ defect, the activation energy for the recovery being $E_A = 0.36 \pm 0.03$ eV.

C. Optical cross section for the generation of the metastable vacancy

In the positron experiments of Fig. 5, the metastable vacancy was generated most effectively at a photon energy of about 1.15 eV. These data can be compared with the infrared-absorption results, which show that the photoquenching is fastest at $E_{ph} = 1.15$ eV. For this comparison, we have calculated the positron-trapping rate at the metastable vacancy, because this parameter is proportional to the vacancy concentration [Eq. (3)].

The positron trapping rate can be calculated as follows. First, we assume that positron trapping at the native Ga vacancies with $\tau_{V_{Ga}} = 260$ ps observed before illumination of the sample remains the same after illumination. Second, we assume that the positron lifetime at the metastable vacancy revealed by illumination is $\tau_{v^*} = 245$ ps (see the discussion above). Then, we can use the positron-lifetime values measured before illumination of the sample and calculate the positron trapping rate at the Ga vacancies from Eq. (7). Therefore, the trapping rate κ_{v^*} at the metastable vacancy can be calculated from the data of Fig. 4 by using Eqs. (4)–(6). The trapping rate and the ir-absorption coefficient are shown in Fig. 7 as functions of the illumination time ($E_{ph} = 1.15$ eV, $\Phi = 10^{14}\ s^{-1}\,cm^{-2}$).

The data in Fig. 7 indicate clearly that the increase of the positron trapping rate and the decrease of the absorption coefficient obey the same dynamics in the stable-metastable transition. For example, the full width at half maximum is about 2500 s in both the curves in Fig. 7. Hence, the amount of metastable vacancies detected in positron experiments is proportional to the fraction of the $EL2$ defects photoquenched to the metastable state.

We can analyze the ir-absorption and positron-lifetime data of Figs. 4 and 5 in terms of the optical cross section for the transition from the stable to the metastable state of $EL2$. As a function of the illumination time t, the concentration of the metastable states $[EL2^*]$ increases as

$$\frac{[EL2^*]}{[EL2]}(t) = 1 - \frac{\alpha(t)}{\alpha(t=0)} = 1 - e^{-(\sigma\Phi)t} , \qquad (10)$$

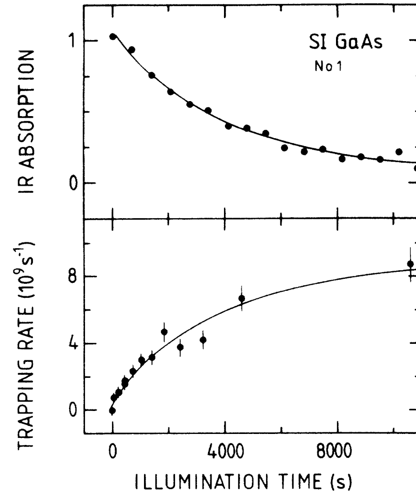

FIG. 7. Normalized absorption coefficient and the positron-trapping rate at the metastable vacancy as a function of illumination time in sample 1. A photon energy of 1.15 eV and a photon flux of $10^{14}\ s^{-1}\,cm^{-2}$ were used in the illumination. The experiments were performed at 25 K.

where α is the absorption coefficient, σ is the optical cross section, and Φ is the photon flux. When the $EL2$ defect dominates the absorption spectrum, the optical cross section σ is the function $\sigma = \sigma^* \sigma_p / (\sigma_p + \sigma_n)$. Here σ_n and σ_p are the optical electron and hole ionization cross sections from the $EL2$ defect level, and σ^* is the cross section for the transition of $EL2$ to the metastable state.[1,33]

The ir-absorption measurements were analyzed by fitting Eq. (10) to the time dependence of the absorption coefficient (e.g., see Fig. 7) with three parameters: $\alpha(t=0)$, $\alpha(t=\infty)$, and σ. The fitted optical cross sections σ for the transition $EL2 \rightarrow EL2^*$ in sample 1 are shown as a function of the photon energy in the upper part of Fig. 8. The photoquenching cross section σ obtains its largest value of $\sigma = 2 \times 10^{-18}\ cm^2$ at the photon energy of $E_{ph} = 1.15$ eV, and the full width at half maximum of the spectrum is about 0.2 eV. Both the shape of the photoquenching peak of Fig. 8 and the absolute values of the optical cross sections are in good agreement with earlier results for the transition $EL2 \rightarrow EL2^*$.[1,33–35] For example, for 1.18-eV photons Vincent, Bois, and Chantre[33] obtained the values of $\sigma_n = 1.5 \times 10^{-16}\ cm^2$, $\sigma_p = 0.6\sigma_n$, and $\sigma^* = 0.08\sigma_n$, which yield the cross section of $\sigma = \sigma^* \sigma_p / (\sigma_p + \sigma_n) = 4.5 \times 10^{-18}\ cm^2$. More recently, Silverberg, Omling, and Samuelson[36] determined the ratio $\sigma_p / (\sigma_p + \sigma_n) = 0.2$ and the cross section $\sigma_n = 1.0 \times 10^{-16}\ cm^2$ for 1.15-eV photons, and by using their values and the relation $\sigma^* = 0.08\sigma_n$ we get $\sigma = 1.6 \times 10^{-18}$ cm,^{2} which is again very close to the results of Fig. 8.

The optical cross section for the generation of the metastable vacancy σ_{v^*} can be calculated from the positron data in the following way. We assume again that positron trapping at the native Ga vacancies with $\tau_{V_{Ga}} = 260$ ps remains the same after illumination, and that the positron lifetime at the metastable vacancy is

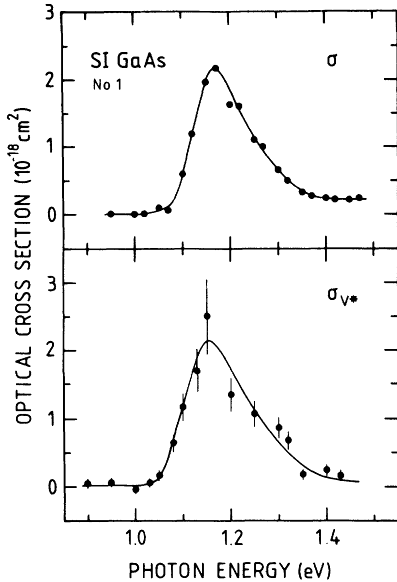

FIG. 8. Optical cross section for the creation of the metastable vacancy as a function of the photon energy in sample 1. The data in the upper part of the figure are obtained from ir-absorption measurements and in the lower part of the figure from positron-lifetime measurements. Measurement temperature was 25 K.

$\tau_{v*}=245$ ps. The positron trapping rate at the metastable vacancy can be calculated from the data of Fig. 5 by using Eqs. (4)–(6). The optical cross section σ_{v*} can then be obtained from an equation similar to Eq. (10):

$$\frac{\kappa_{v*}}{\kappa_{v*}^{\text{tot}}}(t)=1-e^{-(\sigma_{v*}\Phi)t}, \qquad (11)$$

since the positron trapping rate is proportional to the concentration of the metastable vacancy. The parameter κ_{v*}^{tot} in Eq. (11) is the positron trapping rate corresponding to the total concentration of the metastable vacancies. It can be calculated from the saturation of the positron trapping rate in Fig. 7, when the illumination time $t\to\infty$.

The optical cross section for the generation of the metastable vacancy σ_{v*} is shown as a function of the photon energy in the lower part of Fig. 8. As can be seen in the figure, the generation of the metastable vacancy can be induced at photon energies of $E_{\text{ph}}\geq 1.1$ eV. It is most effective at $E_{\text{ph}}=1.15$ eV, at which energy the optical cross section has the value $\sigma_{v*}=2\times10^{-18}$ cm^2. For $E_{\text{ph}}\geq 1.3$ eV the cross section gets very small, but some illumination effect can be obtained up to about 1.5 eV.

The cross section for metastable-vacancy generation is remarkably similar to that obtained for the transition from the stable to the metastable state of the *EL*2 defect in ir-absorption experiments. Both the shape of the photoexcitation spectrum and the absolute level of the optical cross section obtained with the two measurements of Fig. 8 are in perfect agreement with each other. This behavior shows that when *EL*2 is partially photoquenched, the same relative fraction of metastable vacancies appears in the positron experiments. Furthermore, the strong correlation suggests that the disappearance of the ir absorption and the appearance of the metastable vacancy are due to the same optical process. Hence, the metastable vacancy is connected to the metastable state of the *EL*2 defect.

D. Charge of the metastable vacancy

The results of Sec. III D indicate that the illumination-induced increase of the positron average lifetime is strongly temperature dependent: the effect is largest at the lowest measurement temperature of 20 K and it becomes negligible at about 70 K. As explained above, the temperature dependence of the positron trapping is connected to the charge of the vacancy defect. In this section, we shall discuss this temperature effect in more detail.

The positron trapping rate κ_{v*} at the metastable vacancy can be calculated as a function of the measurement temperature using Eqs. (4)–(6). We assume again that before illumination positron trapping takes place at negative Ga vacancies with $\tau_{V_{\text{Ga}}}=260$ ps, and that the positron lifetime at the metastable vacancy is $\tau_{v*}=245$ ps. The calculated temperature dependence of the positron trapping rate κ_{v*} is shown in the lower part of Fig. 9. The trapping rate κ_{v*} has been normalized to its value κ_{v*} (21 K) at the lowest measurement temperature of 21 K. As seen in Fig. 9, the trapping rate κ_{v*} decreases strongly as a function of temperature. Between 21 and 70 K, the change is more than an order of magnitude. Above 70 K, the positron trapping almost disappears as the trapping rate κ_{v*} approaches zero.

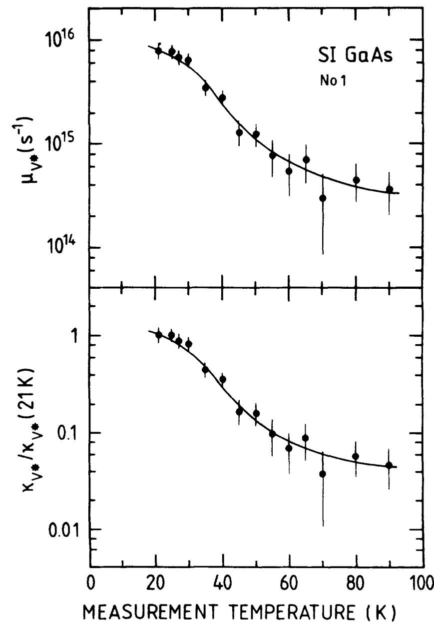

FIG. 9. Positron trapping coefficient and positron trapping rate at the metastable vacancy as a function of measurement temperature. The trapping rate has been normalized to its value at the lowest measurement temperature of 21 K.

The decrease of the positron trapping rate as a function of temperature is typical for negatively charged vacancies.[23-25] At low temperatures of typically $T < 70$ K, the positron trapping coefficient into the negative vacancy varies as $T^{-0.5}$, and at $T = 100-300$ K the temperature dependence becomes roughly as $T^{-1.5}$.[24,25] Hence, the strong decrease of the positron trapping rate κ_{v^*} in Fig. 9 indicates that the charge of the metastable vacancy is negative.

However, the decrease of the trapping rate κ_{v^*} in Fig. 9 is much stronger than the $T^{-0.5}$ dependence found at $T < 70$ K for the Ga vacancies observed before illumination.[37] It is also clearly stronger than in the case of negative vacancy defects in silicon.[23,24] As the temperature dependence of the trapping rate is specific to the detected vacancy defects, the strong decrease of κ_{v^*} thus indicates that (i) the metastable vacancy is different from the native Ga vacancy observed in darkness, and (ii) the metastable vacancy exhibits positron trapping properties which are not typical for isolated negative vacancies. A possible explanation for this could be that the negatively charged metastable vacancy is a part of a larger defect complex, whose total charge is neutral instead of negative.

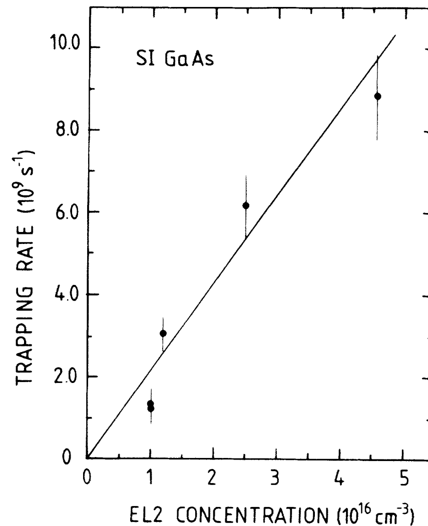

FIG. 10. Positron trapping rate at the metastable vacancy at 25 K as a function of the $EL2$ concentration of the samples. The $EL2$ concentrations indicate the amount of the defect in the neutral charge state $EL2^0$ only.

E. Correlation to the concentration of the $EL2$ defect

The positron trapping rate at a vacancy is proportional to the vacancy concentration [Eq. (3)]. The trapping rates thus give direct information on the relative vacancy concentrations present in different samples. Hence, the concentrations of the metastable vacancies in samples 1–5 can be compared to one another by calculating the positron trapping rates κ_{v^*} at the metastable vacancies in each of the samples.

The positron trapping rates κ_{v^*} can be obtained from the data as in the previous sections by taking $\tau_{v^*} = 245$ ps and by assuming that the Ga vacancies with $\tau_{V_{Ga}} = 260$ ps trap positrons similarly also after illumination. The values of κ_{v^*} at 25 K are shown for samples 1–5 in Fig. 10 as a function of the $EL2$ concentration of the samples. As can be seen in the figure, there is a good correlation between the $EL2$ concentration and the concentration of the metastable vacancies. Hence, we conclude that the concentration of the observed metastable vacancies is proportional to that of the $EL2$ defects. However, it should be noticed that our $EL2$ concentrations indicate only the amount of defects in the neutral charge state $EL2^0$, and only in our sample 5 have EPR experiments shown that $[EL2^0] = [EL2^+] = 1.0 \times 10^{16}$ cm^{-3}.[19]

F. Nature of the metastable vacancy

To summarize the analysis presented in the sections above, we conclude the following. We have observed a metastable vacancy in SI GaAs, when the $EL2$ defect is photoquenched to the metastable state. This vacancy has a smaller open volume than Ga or As vacancies, and it possesses a negative charge. The metastable vacancy is generated with 1.1–1.3-eV light with exactly the same optical cross section as the metastable state $EL2^*$. The metastable vacancy remains in the sample as long as $EL2$ stays in the metastable state, and the vacancy recovers at 120 K with the same annealing kinetics as $EL2^*$. The concentration of the metastable vacancy is proportional to the $EL2$ concentration of the sample. These correlations lead us to conclude that the metastable vacancy is associated with the atomic structure of the metastable state of the $EL2$ defect.

It has been verified that the As antisite defect is a part of the stable state of the $EL2$ defect in GaAs.[1-3] However, there is no consensus whether the As_{Ga} antisite appears in isolation or connected to another defect like an interstitial atom.[1-3] On the other hand, the metastable state of $EL2$ has been found to be optically and electrically inactive, and an electron level connected to it has been observed only under hydrostatic pressure.[4-7] Moreover, no EPR signal has been obtained from the metastable state of the $EL2$ defect, due to its nonparamagnetic neutral charge state.[1-3] Because of this lack of experimental information, the structure of the metastable state has been an open question.

Several atomic models have been proposed also for the transition between the stable and metastable states of $EL2$.[9-14] Most of the models are based on atomic displacements induced by electronic transitions during the $EL2 \rightarrow EL2^*$ transformation. In the model where $EL2$ is an isolated antisite defect As_{Ga}, the As atom relaxes in the metastable state to the interstitial position, leaving a Ga lattice site vacant: $As_{Ga} \rightarrow V_{Ga} + As_i$.[9,10] In another model $EL2$ consists of an As-antisite–As-interstitial pair, in which the As interstitial changes its lattice position in the transition to the metastable state.[12]

The present positron experiments provide direct information on the structure of the metastable state of the $EL2$ defect. The data show that the metastable state contains a vacancy. Further, the results indicate that the va-

cancy has a smaller open volume than Ga or As monovacancies and that the vacancy is connected to a negative charge. These observations are in a perfect agreement with the isolated As_{Ga} model for the *EL*2 defect. In the metastable state the As antisite atom moves towards the interstitial position, leaving a negatively charged Ga vacancy behind. This vacancy has a smaller open volume than the isolated As or Ga vacancies, which explains the low positron lifetime of $\tau_{v*}=245$ ps at the metastable vacancy connected to $EL2^*$. On the other hand, the theoretical models without vacancy defects in the metastable state are in clear contradiction with the present positron data.

Positron lifetimes have been recently calculated in the atomic configuration corresponding to the metastable state of *EL*2 according to the isolated As_{Ga} model.[38] In the calculations, positrons were found to become localized at the V_{Ga}-As_i pair with a lifetime of 250 ps, and the lifetime at the isolated Ga vacancy was 264 ps. These results show that in an atomic configuration such as the close V_{Ga}-As_i pair, the positron lifetime is indeed smaller than in an isolated Ga vacancy. Furthermore, the calculated result of 250 ps coincides very well with the positron lifetime $\tau_{v*}=245$ ps determined in this work for the metastable state of *EL*2.

As the observed metastable vacancy is a part of the structure of $EL2^*$, we can calculate the positron trapping coefficient μ_{v*} at the metastable vacancy from Eq. (3), because the *EL*2 concentration is known. This parameter is presented in sample 1 as a function of the measurement temperature in the upper part of Fig. 9. Notice that the trapping coefficient μ_{v*} is also obtained from the slope of Fig. 10. In Fig. 9 the trapping coefficient decreases with temperature, which indicates that the defect is negative (see Sec. V D). At 20 K the absolute level of $\mu_{v*}=9\times10^{15}$ s^{-1} is comparable to values of $\mu_{v*}\geq10^{16}$ s^{-1} obtained previously for isolated negative monovacancies in Si at 20 K.[23,24] However, the trapping coefficient μ_{v*} decreases very strongly as a function of temperature, and at 50 K its value is already an order of magnitude lower than in the case of a negative monovacancy.[23,24,37] At $T=60-80$ K the trapping coefficient in Fig. 9 seems to saturate at $\mu_{v*}=5\times10^{14}$ s^{-1}, which is close to the values of μ_v at neutral vacancies in semiconductors.[23,24] A possible explanation for this behavior is that the negative vacancy detected in the metastable state is part of a complex, whose total charge is neutral instead of negative. This conclusion would be in agreement with the isolated As_{Ga} model, according to which a negative Ga vacancy is in the metastable state connected to a positive interstitial, but the total charge of the defect is neutral.[9,10]

It should be noticed that the trapping rates in Figs. 7, 9, and 10 are calculated by assuming that the Ga vacancies detected before illumination trap positrons similarly also after illumination. However, it is possible that the charge state of V_{Ga} changes persistently due to the illumination, and the vacancy may even become neutral or positive. If the positron trapping at V_{Ga} disappears completely after illumination, the experimental second lifetime $\tau_2=247$ ps is then the positron lifetime at the metastable vacancy: $\tau_2=\tau_{v*}$. This value differs only by 2 ps from the lifetime $\tau_{v*}=245\pm3$ ps determined by assuming that positron trapping at Ga vacancies remains unaffected. By using $\tau_{v*}=247$ ps the linear relation of Fig. 10 remains similar, but the slope increases by roughly 30% (μ_{v*} at 25 K becomes $\mu_{v*}=1.2\times10^{16}$ s^{-1}). The model used to calculate the positron trapping rates has almost no influence on the optical cross section σ_{v*} shown in Fig. 8. Hence, we can conclude that a possible change of the charge state of V_{Ga} after illumination plays a minor role in the analysis presented in this work.

Finally, we compare the structure of the *EL*2 defect to that of the *DX* center in $Al_xGa_{1-x}As$ compounds. The *DX* center is a well-known defect which is related to an isolated donor impurity like Si or Sn.[39] According to theoretical calculations, the *DX* center has a metastability which closely resembles that of the *EL*2 defect.[40] When the *DX* level is occupied, the donor atom, e.g., Si, is not in the substitutional Ga lattice site but relaxes to the interstitial position, leaving a Ga vacancy behind: $V_{Ga}+Si_i$. Recently, positron trapping at a vacancy-type defect has been observed, when the *DX* level is occupied,[41,42] and the trapping has been attributed to the close-pair configuration $V_{Ga}+Si_i$.[41] This defect complex possesses a smaller open volume than isolated Ga and As vacancies, and the positron lifetime at the *DX* center is 245 ± 5 ps.[41]

The positron results in *EL*2 and *DX* are very similar to each other. In both defects, a vacancy defect is detected in the relaxed configuration. This vacancy has a clearly smaller open volume than isolated elementary vacancies in GaAs. These observations are in good agreement with the theoretical models involving the displacements of the donor atoms (as in the case of *EL*2, a group-IV impurity in the case of *DX*) from the substitutional lattice site to the interstitial position.

VI. CONCLUSIONS

We have investigated the structure of the *EL*2 defect in undoped semi-insulating GaAs by positron-lifetime and Doppler-broadening experiments. Simultaneous infrared-absorption measurements were performed to study the photoquenching of the *EL*2 defect and its relations to the positron-annihilation parameters. The positron experiments were done in darkness at 20–300 K before and after illumination of the sample either with white light or with monochromatic 0.7–1.5-eV light.

After illumination of the undoped GaAs samples with 1.1–1.3-eV light, the positron lifetime at 25 K increases persistently. This effect can be related to the generation of a metastable vacancy defect during the illumination of the sample. The results indicate that this vacancy-type defect has an open volume, which is less than in isolated gallium or arsenic monovacancies. Further, they show that the metastable vacancy is connected to a negative charge.

The generation of the metastable vacancy was found to be most effective with 1.15-eV photons, for which an op-

tical cross section of $\sigma = 2\times10^{-18}$ cm^2 was determined. The photon-energy dependence of this cross section was investigated, and a full width at half maximum of about 0.2 eV was obtained for the peak centered around 1.15 eV. In annealing experiments performed after illumination, the metastable vacancy was found to disappear at 120 K.

All the properties listed above for the metastable vacancy coincide well with those of the metastable state of the *EL*2 defect. Furthermore, the concentration of the metastable vacancies is proportional to the *EL*2 concentration of the samples. We thus conclude that the observed metastable vacancy is involved in the atomic configuration of the metastable state of the *EL*2 defect. Hence, the results indicate that the metastable state of *EL*2 contains a vacancy, whose open volume is less than in isolated Ga and As vacancies. This observation is in good agreement with the isolated As antisite model for the structure of *EL*2. In this model, the As antisite atom relaxes in the metastable state towards the interstitial position, leaving a metastable Ga vacancy behind: $As_{Ga} \rightarrow V_{Ga} + As_i$.

ACKNOWLEDGMENTS

We would like to thank M. Spaeth and C. Schwab for the GaAs samples and R. Krause and L. Liszkay for their help in some of the experiments in this work. We are also grateful for discussions with J. Mäkinen, R. M. Nieminen, and M. J. Puska.

[1]G. M. Martin and S. Makram-Ebeid, in *Deep Centers in Semiconductors,* edited by S. T. Pantelides (Gordon and Breach, New York, 1986), Chap. 6.

[2]M. O. Manasreh, D. W. Fischer, and W. C. Mitchel, Phys. Status Solidi B **154**, 11 (1989).

[3]J. C. Bourgoin, H. J. von Bardeleben, and D. Stiévenard, J. Appl. Phys. **64**, R65 (1988).

[4]M. Baj, P. Dreszer, and A. Babinski, Phys. Rev. B **43**, 2070 (1991).

[5]P. Dreszer, M. Baj, and K. Korzeniewski, in *Defects in Semiconductors,* Vols. 83–87 of Materials Science Forum, edited by G. Davies, G. G. DeLeo, and M. Stavola (Trans Tech, Aedermannsdorf, 1992), p. 875.

[6]T. W. Steiner, M. K. Nissen, S. M. Wilson, Y. Lacroix, and M. L. W. Thewalt, Phys. Rev. B **47**, 1265 (1993).

[7]D. Stiévenard, C. Delerue, G. Brémond, G. Guillot, R. Azoulay, H. J. von Bardeleben, J. C. Bourgoin, J. C. Portal, and E. Ranz, in *Defects in Semiconductors* (Ref. 5), p. 911.

[8]E. R. Weber, H. Ennen, U. Kaufman, J. Windscheif, J. Schneider, and T. Wosinski, J. Appl. Phys. **53**, 6140 (1982); E. R. Weber and J. Schneider, Physica B and C **116B**, 398 (1983).

[9]J. Dabrowski and M. Scheffler, Phys. Rev. Lett. **60**, 2183 (1988); Phys. Rev. B **40**, 10 391 (1989).

[10]D. J. Chadi and K. J. Chang, Phys. Rev. Lett. **60**, 2187 (1988).

[11]G. A. Baraff and M. Schlüter, Phys. Rev. Lett. **55**, 2340 (1985).

[12]H. J. von Bardeleben, D. Stiévenard, D. Deresmes, A. Huber, and J. C. Bourgoin, Phys. Rev. B **34**, 7192 (1986).

[13]J. F. Wager and J. A. van Vechten, Phys. Rev. B **35**, 2330 (1987).

[14]G. Wang, Y. Zou, S. Benakki, A. Goltzene, and C. Schwab, J. Appl. Phys. **63**, 2595 (1988).

[15]*Positrons in Solids,* edited by P. Hautojärvi, Topics in Current Physics Vol. 12 (Springer-Verlag, Heidelberg, 1979).

[16]*Positron Solid State Physics,* edited by W. Brandt and A. Dupasquier (North-Holland, Amsterdam 1983).

[17]R. Krause, K. Saarinen, P. Hautojärvi, A. Polity, G. Gärtner, and C. Corbel, Phys. Rev. Lett. **65**, 3329 (1990).

[18]P. Hautojärvi, K. Saarinen, L. Liszkay, C. Corbel, and C. LeBerre, in *Defects in Semiconductors* (Ref. 5), p. 923.

[19]C. Schwab and A. Golzené (private communication).

[20]G. M. Martin, Appl. Phys. Lett. **39**, 747 (1981).

[21]G. A. Baraff and M. A. Schlüter, Phys. Rev. B **45**, 8300 (1992).

[22]D. W. Fischer, Phys. Rev. B **37**, 2968 (1988).

[23]J. Mäkinen, C. Corbel, P. Hautojärvi, P. Moser, and F. Pierre, Phys. Rev. B **39**, 10 162 (1989).

[24]J. Mäkinen, P. Hautojärvi, and C. Corbel, J. Phys. Condens. Matter **3**, 7217 (1991).

[25]M. J. Puska, C. Corbel, and R. M. Nieminen, Phys. Rev. B **41**, 9980 (1990).

[26]R. N. West, in *Positrons in Solids* (Ref. 15) , p. 89.

[27]K. Saarinen, P. Hautojärvi, P. Lanki, and C. Corbel, Phys. Rev. B **44**, 10 585 (1991).

[28]C. Corbel, M. Stucky, P. Hautojärvi, K. Saarinen, and P. Moser, Phys. Rev. B **38**, 8192 (1988).

[29]C. Corbel, F. Pierre, K. Saarinen, P. Hautojärvi, and P. Moser, Phys. Rev. B **41**, 10 632 (1990).

[30]C. Corbel, F. Pierre, K. Saarinen, P. Hautojärvi, and P. Moser, Phys. Rev. B **45**, 3386 (1992).

[31]M. Puska, S. Mäkinen, M. Manninen, and R. M. Nieminen, Phys. Rev. B **39**, 7666 (1989).

[32]K. Saarinen, S. Kuisma, P. Hautojärvi, C. Corbel, and C. LeBerre, Phys. Rev. Lett. **70**, 2794 (1993).

[33]G. Vincent, D. Bois, and A. Chantre, J. Appl. Phys. **53**, 3643 (1982).

[34]M. O. Manasreh and D. W. Fisher, Phys. Rev. B **40**, 11 756 (1989).

[35]E. Christoffel, A. Goltzene, and C. Schwab, J. Appl. Phys. **66**, 5648 (1989).

[36]P. Silverberg, P. Omling, and L. Samuelson, Appl. Phys. Lett. **52**, 1689 (1988).

[37]More details of the temperature dependence of the positron trapping coefficient in GaAs will be published separately.

[38]K. Laasonen, M. Alatalo, M. J. Puska, and R. M. Nieminen, J. Phys. Condens. Matter **3**, 7217 (1991).

[39]P. M. Mooney, J. Appl. Phys. **67**, R1 (1990).

[40]D. J. Chadi and K. J. Chang, Phys. Rev. Lett. **61**, 873 (1988).

[41]J. Mäkinen, T. Laine, K. Saarinen, P. Hautojärvi, C. Corbel, V. M. Airaksinen, and P. Gibart, Phys. Rev. Lett. **71**, 3154 (1993).

[42]R. Krause-Rehberg, Th. Drost, A. Polity, G. Roos, G. Pensl, D. Volm, B. K. Meyer, G. Bischopink, and K. W. Benz, Phys. Rev. B **48**, 11 723 (1993).